Acoustic anemometry and thermometry

B. M. Brecht, A. Raabe and A. Ziemann

Abstract

Acoustic travel-time measurement is a method for remote sensing of the atmosphere. The temperature-dependent sound speed as well as the flow field can be detected by measuring the travel time of a defined acoustic signal between a sound source and a receiver when the distance between them is known. In this study the properties of the flow field are reconstructed using reciprocal sound rays to separate the direction-independent sound speed from the effective sound velocity including the flow velocity component in direction of the sound path. The measurements are taken on a horizontal scale of about 2 m x 2 m. By measurements in interiors, where no flow of air exists, the temperature can be determined with an accuracy of 0.6°C and the flow component in direction of the sound path with an accuracy of 0.3 m/s. If flow of air exists the measurements gets complicated because the phase shifts, which have been detected by the receivers, cannot be corrected like it was possible without the influence of flow.

1 Introduction

The motivation to do travel-time tomography in the atmosphere is to get consistent, measured data to validate numerical atmosphere-models like Large-Eddy simulations (LES), which has become a common tool to investigate several questions of the micro scale structure of the atmosphere (Arnold et al., 2003). Therefore area or volume-averaged values are needed, which the travel-time tomography provides. Conventionally such spatially data have been provided by point measurements and additional interpolation or up-scaling algorithms. Travel-time tomography provides this data directly with a high spatial and temporal resolution (Arnold et al., 2003).

Acoustic tomography exists a long time. At first Spiesberger and Fristrup (1990) verified an experimental application of a tomographic horizontally–sliced scheme to the atmospheric surface layer. They described a method for passively locating the calls of animals. Wilson and Thomson (1994) also verified this method with the concentration on the characteristics of the atmosphere (Tetzlaff et al., 2002). Then the work with acoustic tomography has started at the Institute of Meteorology of the Leipzig University (LIM). Arnold et al. (1999), Raabe et al. (2001) and Ziemann et al. (1999 a, b) demonstrated the applicability of acoustic travel-time tomography to detect absolute values of the temperature and the wind vector with no additional information apart from air humidity (Tetzlaff et al., 2002).

There were several projects relating to acoustic travel-time tomography at the LIM, inter alia the STINHO-project, a field-campaign at the boundary layer field site of the

Meteorological Observatory Lindenberg of the German Meteorological Service in the summer of 2002. The intention was to compare conventional meteorological point and vertically integrated measurements with area-covering air flow observations and numerical simulations. To observe horizontally variable flow and temperature fields above a heterogeneous land surface they used, inter alia, travel-time tomography (Raabe et al., 2005). In this project the researched area had a range of 300 m x 440 m. Besides the application on meteorological boundary layer field sites to get consistent data to validate numerical atmosphere-models like LES the method of acoustic travel-time tomography can be used on other questions as well. It can also be applied on shorter distances between the sound source and receiver, like only a few meters. This work began on the LIM using an apparatus that worked with audible sound signals and was suitable for wind and temperature measurements on a scale of 1 m (Barth et al., 2007). The travel times between a sound source and a sound receiver were detected with a correlation technique, where the travel time was that time, in which the correlation between the transmitted and received signal was the biggest. On these shorter distances it is possible to measure flow patterns in wind channels or the flow in atmosphere-chambers or halls. Another field of application in which travel-time measurements could be useful is in Greenhouses, because the air speed distribution is a key factor influencing heat and mass transfer there. Wang et al. investigated the air speed profiles in the centre of a naturally ventilated greenhouse with a tomato crop by means of a customized multi-point two dimensional sonic anemometer system and the experimental results showed that air speed was linearly dependent both on external wind speed and greenhouse ventilation flux (Wang et al., 1999). For this acoustic travel-time tomography could be used as well.

Aim of this work is to develop a progress of the acoustic travel-time measurement on a horizontal scale of about 2 m x 2 m, like Barth did, with a start-stop measuring technique. The presented method uses ultrasound and can carry up to ten measurements per second. A fact, that is especially for measurements in turbulent flows of advantage.

2 Basics of acoustic travel-time measurements

Sound waves, or acoustic waves, are longitudinal waves. Sound is propagated by the alternating adiabatic compression and expansion of the medium (Holton, 2004).

The speed of sound in a medium is determined by its characteristics, that means in the atmosphere the temperature, the moisture and the flow vector of the air.

2.1 Speed of sound in gases

For an ideal gas, which is a valid idealization for air (Pierce, 1994), and the assumption of adiabatic change of condition by the propagation of sound, the adiabatic speed of sound c_L results from the pressure p and the density ρ to

$$c_{\mathrm{L}} = \sqrt{\gamma_{\mathrm{dry}} R_{\mathrm{dry}} T}\,, \tag{2.1}$$

where γ_{dry} is the ratio of the specific heat capacities for constant pressure to constant volume, R_{dry} is the specific gas constant for dry air and T the air temperature in Kelvin. The sound velocity c_{L} is also called Laplace's speed of sound. The specific gas constant R_{dry} amounts 287.05 J kg^{-1} K^{-1} and γ_{dry} can be assumed to be constant for air in the temperature range of interest and is equal to 1.4 (Pierce, 1994).

The presence of water vapor changes both the gas constant and the specific heat capacity. The resulting equation for Laplace's speed of sound, depending on the specific humidity q, becomes

$$c_{\mathrm{L}} = \sqrt{\left[(1 + 0.51q)\gamma_{\mathrm{dry}} \cdot R_{\mathrm{dry}} \cdot T\right]}\,. \tag{2.2}$$

The temperature has a bigger influence on the speed of sound as the humidity. For the using here the moisture is not negligible, but it is sufficient to make the assumption of a constant value.

In a real atmosphere the velocity of sound depends also on the flow of air. This dependence is vectorial and not scalar, like that from the temperature and the moisture. To describe the influence of the wind vector **v** on the sound speed, the effective speed of sound is often used:

$$c_{\mathrm{eff}} = c_{\mathrm{L}}\left(T_{\mathrm{av}}(\mathbf{r}, t)\right) + \mathbf{v}(\mathbf{r}, t) \cdot \mathbf{s} = c_{\mathrm{L}}\left(T_{\mathrm{av}}(\mathbf{r}, t)\right) + v_{\mathrm{ray}}. \tag{2.3}$$

Here **s** represents an unit vector, which is tangential to the sound path from the sound source to the receiver (Ostashev, 1997), **r** represents the space vector, t the time and v_{ray} describes the projection of the flow vector to the direct line between the sound source and the receiver and therefore the flow component in the direction of the sound ray. Consequently c_{eff} has both a temperature-depending part (c_{L}) and a flow-depending part (v_{ray}). Therefore the vectorial influence of the wind is attributed to the scalar addition of Laplace's sound velocity c_{L} and the wind component in the direction of the sound ray v_{ray}. Equation 2.3 is an approximation, because the unit vector **s** is bending with the influence of wind. The approximation is valid if the properties of the ambient medium (**v**) changes much slower than the characteristically time of the energy transport (c_{eff}).

2.2 Separation of the temperature and flow dependence

To separate the scalar influence of the temperature and the directional influence of the flow vector on the speed of sound there are used bidirectional, nearly reciprocal, sound paths. The application of this principle is used, e.g., by ultrasonic anemometers. Therefore reciprocal sound propagation can be assumed. Laplace's sound speed can be

derived by adding the forward and backward travel times (Equation 2.4). The flow's velocity component along the sound ray path can be derived by subtracting the forward and backward travel times (Barth, 2007). The resulting equations look like the following:

$$c_{\mathrm{L}} = \frac{d}{2}\left(\frac{1}{\tau_{0,\mathrm{forward}}} + \frac{1}{\tau_{0,\mathrm{backward}}}\right), \tag{2.4}$$

$$v_{\mathrm{ray}} = \frac{d}{2}\left(\frac{1}{\tau_{0,\mathrm{forward}}} - \frac{1}{\tau_{0,\mathrm{backward}}}\right). \tag{2.5}$$

Here d is the distance between a sound source and receiver and τ_0 is the travel time of a sound signal.

3 The measuring system

To get the effective speed of sound it is necessary to have exact information both about the travel time of a sound wave between the sound source and receiver and the distance between them. The more exact the information about the travel time and the path length between the sound source and receiver the more precisely is the determination of the meteorological parameters. From the travel time of a sound signal Laplace's sound speed c_{L} and therefore both the temperature T and the flow vector **v** can be determined by using reciprocal straight-lined sound paths and knowledge about the length of these paths.

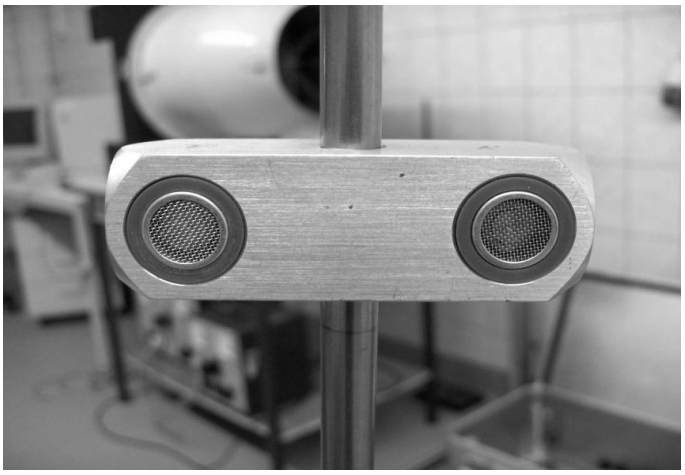

Fig. 3.1: Transmitter-receiver couple

3.1 Properties of the measuring instrument

The measuring equipment consists of a data logger with eight channels, a notebook and eight transmitter-receiver couples (Figure 3.1). The data logger is connected with the notebook, which contains a program to control the measurement and makes it possible to change a few measuring parameters. The measuring parameters which can be changed are the transmitting power and the trigger threshold of the signal. It is also possible to take the mean of the received travel times up to ten times automatically. The transmitter-receiver couples detect travel-times on bidirectional (reciprocal sound propagation can be assumed) ways at two different planes and between these two planes. They have a club-directional characteristic. An arrangement for the transmitter-

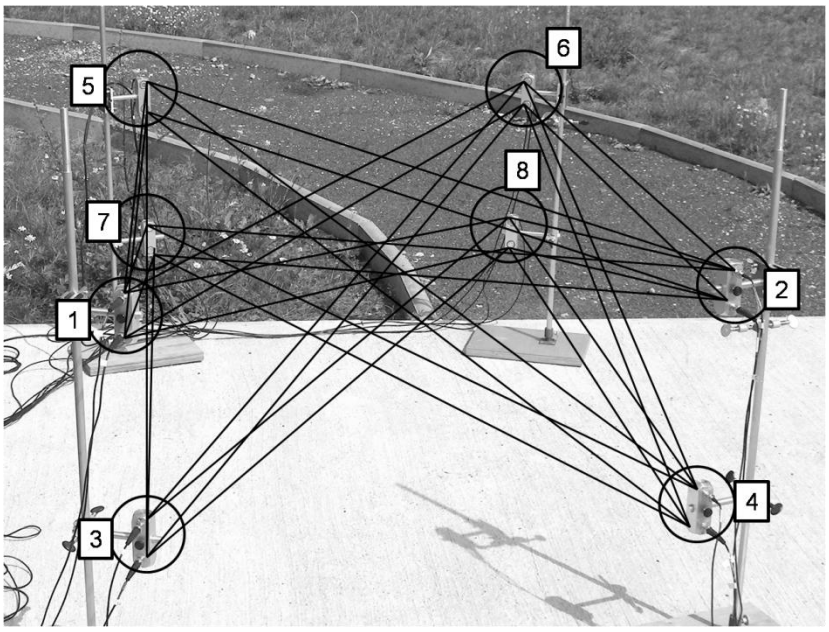

Fig. 3.2: Arrangement of the 8 transmitter and receiver couples

receiver couples is shown in figure 3.2. The transmitter-receiver couples number 1, 2, 3 and 4 always transmits respectively receives sound rays to/from the transmitter-receiver couples 5, 6, 7 and 8. The transmitting frequency is in the ultrasonic range and is 40 kHz ± 1 kHz. Therefore it is possible to detect the travel-times with a high temporal resolution. The current configuration of the measuring instrument detects one value of travel time every three seconds. It is also possible to get an average of ten values per three seconds.

3.2 Detection of the travel-time

The detection method of the travel-times is a so called "Start-Stop-Measurement". The electronic transmitting impulse is a sinus burst with five oscillations. One period has 25 µs. The wave peaks arriving at the receiver have, after filtering and rectification, an interval of 12.5 µs. The transmitting power can be set between 0 and 10 volts. There is a trigger-threshold at the receiver, which can be set between 0 and 2.5 volts. If a sinus burst is sending out, the travel-time begins to start. The measurement stops, when the first wave peak, which is higher than the trigger-threshold, is detected by the receiver. This period of time is the travel time (Figure 3.3). The order of the measurement is as follows: At first transmitter 1 sends a signal, which is received by receiver 5, 6, 7 and 8. Then transmitter 2 sends a signal to receiver 5, 6, 7 and 8, then 3 and 4 to 5, 6, 7 and 8. Afterwards transmitter 5 sends to receiver 1, 2, 3 and 4, then 6, 7 and 8 to 1, 2, 3 and 4. That gives 8·4 = 32 travel times. The travel time will be shorter for both if the trigger

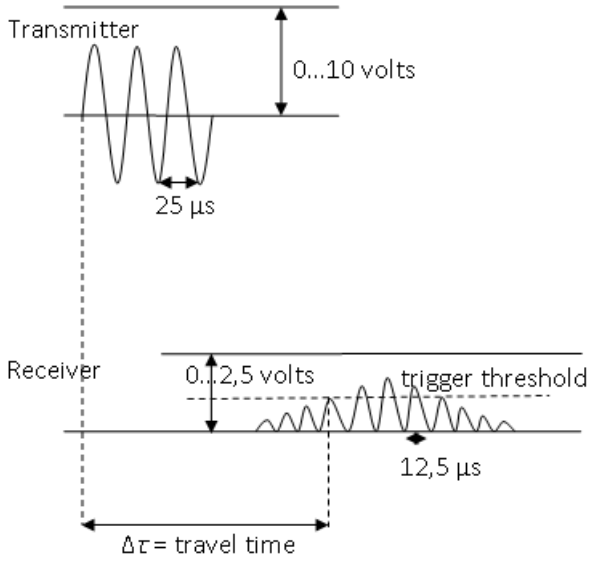

Fig. 3.3: Principle of the travel-time detection

threshold would be reduced, because the waves would be detected earlier and if the transmitting power would be raised, because the amplitudes of the waves would be higher and consequently the trigger threshold would be arrived earlier.

3.3 Measuring accuracy

The measuring accuracy depends in principle on the exactness in the determination of the distance and the travel time between a transmitter and receiver. The path length was determined with a ruler and the accuracy was assumed to $u(d) = 5$ mm. By the following equation

$$u_{\max}(Y) = \left|\frac{\partial Y}{\partial X_1}\right| u(X_1) + \cdots + \left|\frac{\partial Y}{\partial X_{\mathrm{m}}}\right| u(X_{\mathrm{m}}), \qquad \textbf{(3.1)}$$

by equation 2.2, with the precondition that there is no flow of air (**v** = 0) and the assumption that the travel time has no error ($u(\tau_0) = 0$) the maximal error for the temperature results to

$$u_{\max}(T) = \left|2 \cdot \frac{d}{{\tau_0}^2 \cdot \gamma_{\mathrm{dry}} \cdot R_{\mathrm{dry}} \cdot (1 + 0.51 \cdot q)}\right| \cdot u(d). \qquad \textbf{(3.2)}$$

Here d means the path length between a transmitter and receiver, τ_0 is the travel time of the sound wave, γ_{dry} the ratio of the specific heat capacities for dry air, R_{dry} the specific gas constant for dry air and q the specific humidity. The resulting temperature inaccuracy is $u_{\max}(T) = \pm$ 1,5°C using a path length of 2 m and the following ambient conditions: $T = 20$°C, $p = 1000$ hPa and *r.h.* (relative humidity) = 70 %.

The travel-time accuracy is closely connected to the error of the dead time of the system. There are two modes of dead time error.

The first one is the electronic dead time, which is an error that is based on processes inside the electronic system. This error is of the dimension of maximal 10 µs, but not exactly determinable, which corresponds to a temperature error of almost 1°C by a path length of 2 m and the same ambient conditions as mentioned above.

The second dead-time error takes place because the first wave peak, which arrives at the trigger threshold, is generally not by the first wave, which was transmitted by the transmitter and would represent the real travel time (Figure 3.3). This error ensues probable from a delayed oscillating phase and from the noise. But it has to be investigated further. Therefore a travel-time error of n phase shifts appears, which is in the range of $n \cdot 12.5$ µs and leads to a temperature error of $n \cdot 1.25$°C by a path length of 2 m and the same ambient conditions as mentioned above. The problem is that it is not possible to find out which wave peak was detected; therefore it is impossible to determine the travel time with a satisfying accuracy. The resulting dead time error therefore is $10 \pm n \cdot 12.5$ µs. That matches a temperature error of $u_{\max}(T) = 1$°C $\pm\, n \cdot 1.25$°C.

The dead time error is a systematically error, which theoretically could be corrected with a measurement varying the path lengths between the transmitter and receiver and build a linear fit to get the dead time. The problem by changing the path lengths by a fixed setting for the transmitting power and the trigger threshold is that other wave peaks will always be detected. This would distort the measurement. For example, by changing the distance between transmitter and receiver from a higher to a lower length the receiver will detect the travel time one or more phase shifts before, because the amplitude which arrives the receiver is higher for shorter path lengths. Therefore this error cannot be corrected.

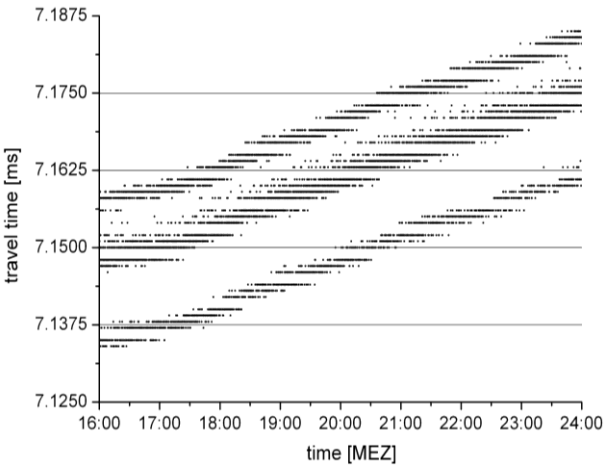

Fig. 3.4: Example for a travel-time measurement from transmitter 1 to receiver 6 (path 1_6). There are three phase shifts visible.

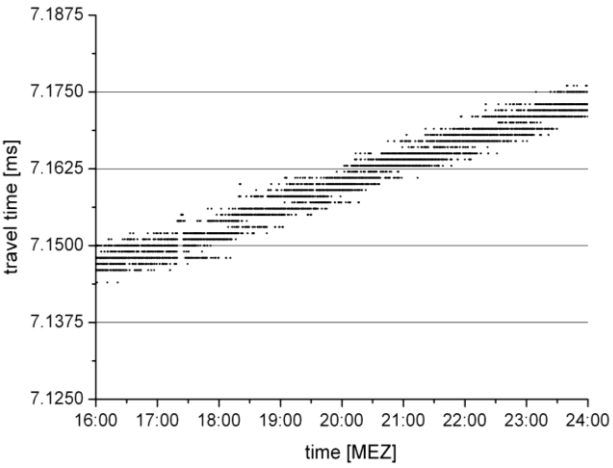

Fig. 3.5: The same travel-time measurement as shown in figure 3.4. The three phase shift beams are summarized to one.

The consequence of these unsatisfactory errors is to make relative measurements which require information about the temperature, the relative humidity, the air pressure (a constant value of 1000 hPa can be assumed) and the flow of air at a starting time. In a period of time, in which these measurements are constant and uniform, the effective speed of sound can be calculated by equation 2.2. With the assumption that $c_L = c_{eff}$ ($\mathbf{v} = 0$) and the equation

$$c_{\text{eff}} = \frac{d}{\tau_0} <=> d = c_{\text{eff}} \cdot \tau_0 \qquad \textbf{(3.3)}$$

there can be new path lengths calculated, which deletes occurring path-length and travel-time errors. The variable d is the new path length and τ_0 is the measured travel time including the path-length and travel-time errors. The accuracy of the relative measurements is, of course, only so exact like the measurements from the parallel measurements of the temperature, the relative humidity and the air flow are.

Another problem that leads to an inaccuracy in the measurement is that there are several phase shifts for one measurement setting (transmitting-power and trigger-threshold). This problem is shown in figure 3.4. If there is no air flow it is possible to

summarize the phase shifts by adding and subtracting the several phase shift beams to one phase shift beam (Figure 3.5). If there is an air flow this procedure is impossible.

4 Results

The measurements represented here exemplarily were made in a room with no flow of air. Figure 4.1 shows the temperature of the acoustic measurement of path 1_6 (transmitter 1 to receiver 6) and the temperature of the humitter from VAISALA, which supplies parallel information about the temperature and the relative humidity, versus time. The dispersion of these both measurements is nearly the same and it seems to be possible to determine the temperature with an accuracy of 0.6°C.

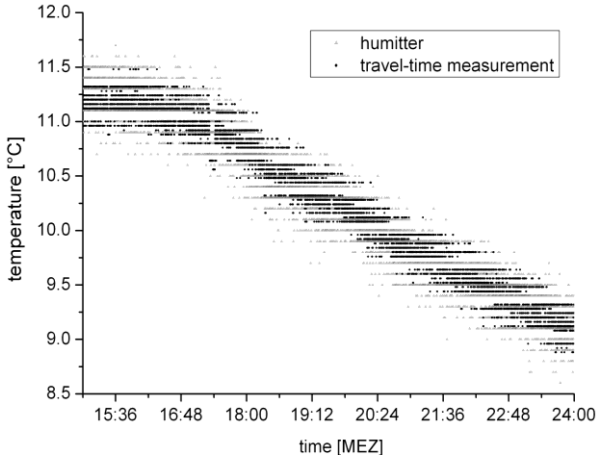

Fig. 4.1: Temperature of path 1_6 (black points) and temperature of the humitter (grey triangles) versus time.

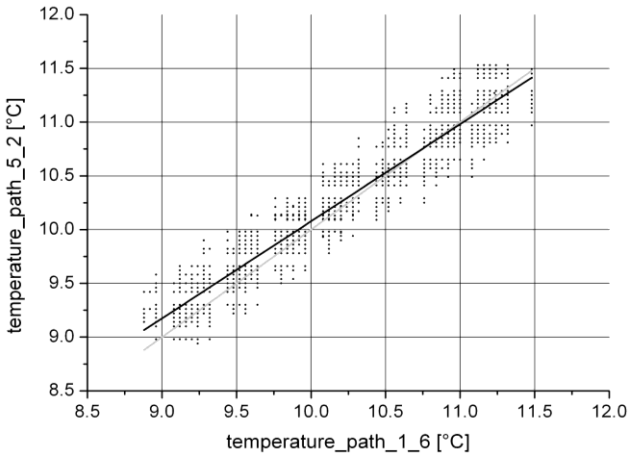

Fig. 4.2: Temperature of path 1_6 versus temperature of path 5_2 with a linear regression line (black line). The regression coefficient is $R^2 = 0.92$.

Therefore temperature oscillations greater 0.6°C should be detectable. Figure 4.2 shows the correlation between the acoustic measurement of path 1_6 and path 5_2. It shows a good correlation with a regression coefficient of $R^2 = 0.92$. In a room without air flow the value of v_{ray} should be zero, because the travel-times forward and backward should be the same for the same path length (Equation 2.5). Figure 4.3 shows such a case. The flow component in the direction of the sound ray v_{ray} of path 1_6_1 (forward path 1_6 and backward path 6_1) fluctuates here about maximal ± 10 cm/s around zero, which is adequately a good result. The sensitivity of this

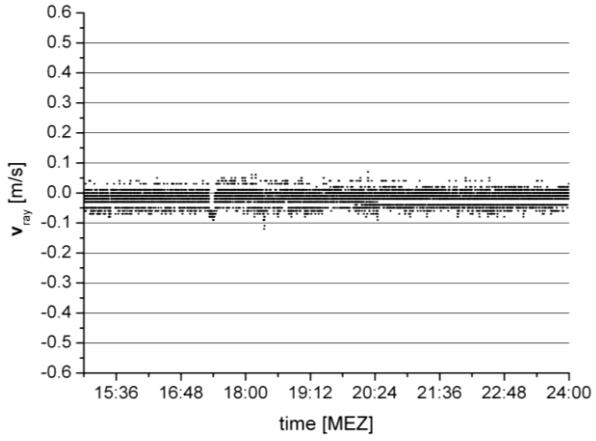

Fig. 4.3: The flow component in the direction of the sound ray v_{ray} of path 1_6_1 versus time.

measurement method could be estimated about the dispersion to ~ 0.2 m/s.
The displayed results provided up to now were all in absence of the flow of air. If a wind velocity greater zero exists, the phase shift beams, seen in figure 3.4, are not distinguishable. Consequently it is not possible to use the same procedure for the temperature analysis (see figures 3.4 and 3.5). Thus the results for the wind component along ray path and therefore for the resulting wind vector are unsatisfactory, as seen in figure 4.4. The figure shows a measurement in a wind channel. A directional-independent thermo-anemometer was used to evaluate the acoustic measurement by comparing the results. In the first minutes there were no flow of air and four phase shift beams can be seen (see figure 4.4). After the wind channel was switched on (from 11:38 – 13:00 with a constant voltage and from 13:00 – 14:25 with a higher constant voltage) no more phase shift beams can be seen, so it is impossible attributing the high dispersive values to values with lower dispersion. But the right tendency of the wind vector in comparison with the anemometer measuring can be seen. This shows that this method could work with a satisfying accuracy if there would be no phase shifts in the travel-time detection.

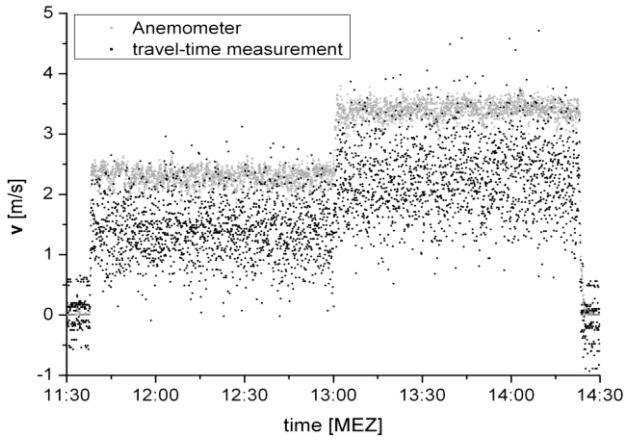

Fig. 4.4: Wind channel measurement: black dots show the acoustic measurement of path 2_6_2 and grey triangles show the measurement of an anemometer to have a comparison. The voltage values of the wind channel were constant from both 11:38 – 13:00 and 13:00 – 14:25.

5 Conclusions

As shown in chapter 4 it is possible to determine the temperature and flow component in the direction of the sound ray v_{ray} with a good accuracy if there is no flow of air. The temperature T has an accuracy of 0.6°C (figure 4.1), which is in the range of the accuracy of the humitter, and v_{ray} has an accuracy of ~ 0.2 m/s (figure 4.3). The problems are the several phase shift beams which occur at the measurements. If the wind velocity is greater zero the phase shift beams cannot be corrected. Therefore it must be the aim to change the measuring instrument in such a way that the phase shifts won't occur any more. Where the changes in the electronic system have to follow exactly is not sure yet, it has to be tested and investigated further. Another expansion of the measuring equipment could be a higher temporal resolution like the display of 10 values of the travel-time per three seconds without averaging. A possible application of this method is a flow balance measurement of incoming and outcoming flow of gases, e.g. by windows or over areas of lysimeters. By a high temporal

resolution of the temperature and wind field it could be also possible to solve micro-scale turbulence in the atmosphere.

Acknowledgements

We would like to thank both Manuela Barth for the good advices and suggestions and Frank Weisse for the technical support and also for the discussions and explanations about the measuring instrument.

References

Arnold, K., Ziemann, A., Raabe, A. and Spindler, G., 2003: Acoustic tomography and conventional meteorological measurements over heterogeneous surfaces. Meteorol. Atmos. Phys. 85, 175-186

Barth, M.:2009: Akustische Tomographie zur zeitgleichen Erfassung von Temperatur- und Strömungsfeldern. Wissenschaftliche Mitteilungen, Institute of Meteorology from the Universiy of Leipzig, Volume 44

Barth, M., Raabe A., Arnold, K., Resagk, C. and du Puits, R., 2007: Flow field detection using acoustic travel time tomography. Meteorologische Zeitschrift, Vol. 16, No. 4, 443-450

Holstein, P., Raabe, A., Müller, R., Barth, M., Mackenzie, D. and Starke, E., 2004: Acoustic tomography on the basis of travel-time measurement. Meas. Sci. Technol. 15, 1420–1428

Holton, J. R., 2004: An Introduction to Dynamic Meteorology. Fourth Edition. Elsevier Academic Press, 535 S.

Ostashev, V. E., 1997: Acoustics in Moving Inhomogeneous Media. E & FN Spon, London, Weinheim, New York, Melbourne, Madras, 259 S.

Pierce, A. D., 1994: Acoustics – An Introduction to Its Physical Principles and Applications. Published by the Acoustical Society of America through the American Institute of Physics, 678 S.

Raabe, A., Arnold, K., Ziemann, A., Beyrich, F., Leps, J.-P., Bange, J., Zittel, P., Spiess, T., Foken, T., Göckede, M., Schröter, M., and Raasch, S., 2005: STINHO – Structure of turbulent transport under homogeneous surface consitions – part 1: The micro-α scale field experiment. Meteorologische Zeitschrift, Vol. 14, No. 3, 315-327

Tetzlaff, G., Arnold, K., Raabe, A. and Ziemann, A., 2002: Observations of area averaged near-surface wind- and temperature-fields in real terrain using acoustic travel time tomography. Meteorologische Zeitschrift, Vol. 11, No. 4, 273-283

Wang, S., Boulard, T., Haxaire, R., 1999: Air speed profiles in a naturally ventilated greenhouse with a tomato crop. Agricultural and Forest Meteorology 96, S. 181-188